An Effective Time Varying Delay Estimator Applied to Surface Electromyographic Signals

Gia Thien Luu[1(✉)], Abdelbassit Boualem[2], Philippe Ravier[2], and Olivier Buttelli[2]

[1] Department of Physics, Posts and Telecommunications Institute of Technology, Ho Chi Minh City, Vietnam
lgthien@ptithcm.edu.vn
[2] University of Orleans, Orleans, France
{philippe.ravier,olivier.buttelli}@univ-orleans.fr

Abstract. Muscle Fiber Conduction Velocity (MFCV) can be calculated from the time delay between the surface electromyographic (sEMG) signals recorded by electrodes aligned with the fiber direction. In order to take into account the non-stationarity during the dynamic contraction (the most daily life situation) of the data, the developed methods have to consider that the MFCV changes over the time, which induces time varying delays and the data is non-stationary (change of Power Spectral Density (PSD)). In the present paper, the problem of time varying delay (TVD) estimation is considered using a parametric method. First, the polynomial model of TVD has been proposed. Then, the TVD model parameters are estimated by using a maximum likelihood estimation (MLE) strategy solved by a stochastic optimization technique, called simulated annealing (SA). The Monte-Carlo simulation results show that the estimation of both the model parameters and the TVD function is unbiased and that the variance obtained is close to the Crammer-Rao Lower Bound (CRLB). We also compared the performance of the proposed method with non-parametric approaches. The results indicate that the proposed method outperform the non-parametric one.

Keywords: Electromyography · Time-varying delay
Muscle Fiber Conduction Velocity · Non-stationarity
Maximum likelihood estimation · Simulated annealing (SA) · CRLB

1 Introduction

Muscle Fibers Conduction Velocity (MFCV) is an interesting physiological indicator, *e.g.* for monitoring neuro-muscular degenerative diseases [1] and also for the assessment of pain in the case of fibromyalgia [7]. This indicator was also widely used for fundamental studies on motor control, *i.e* Motor Unit (MU)

P. Cong Vinh et al. (Eds.): ICCASA 2017/ICTCC 2017, LNICST 217, pp. 214–225, 2018.
https://doi.org/10.1007/978-3-319-77818-1_21

recruitment modality based on force levels; study of fatigue [13,19] whose applications include both the medical field that the physiology of the exercise and ergonomics. MFCV can be estimated from intramuscular or surface electromyography recordings [14]. In this work, we are only interested in surface EMG signals (sEMG).

In the case of dynamics contraction (the most daily situation), Farina et *al.* [6] adapted the maximum likelihood estimator to short analysis intervals. However the resulting approach does not provide an instantaneous delay estimation [17]. In [9,10,17], the time frequency and time scale approaches were developed for the problem of time varying estimation for each instant. In such cases, the TVD model choice is not critical since the investigated methods are independent of TVD model. However, the obtained performance suffers from high noise levels and the performance of these methods are depends on the PSD shapes of the sEMG signal.

Optimal TVD estimators can be derived with Maximum-Likelihood estimation (MLE) method. However, in such case, we have to estimate N parameters, the time of calculation is too much. In [12], we proposed a polynomial model for the TVD and adapted the maximum likelihood estimation for the short time to estimate the model parameters. A deterministic optimization was used into the sliding window to solve the optimization problem. However, this technique does not guarantee the global optimization. To solve this problem, in present paper, we proposed an stochastic optimization called stimulated annealing technique combined with the MLE method.

The paper is organized as follows. In Sect. 2, the models of signals and TVD will be defined. In Sect. 3, the MLE method two channels will be derived. Section 4 presents the simulation results with synthetic sEMG compared with the CRLB which was derived in [11]. In Sect. 5, we conclude the paper.

2 Model of sEMG Synthetics Signals

In this section, we first present an analytical model for two-channel sEMG acquired signals, and then a generating model of synthetics EMG signals. This model is helpful for statistical performance studies.

2.1 Signal Model

Considering the sEMG signal s(n) propagating between channel 1 and channel 2, a simple analytical model of two observed signals $x_1(n)$ and $x_2(n)$ in a discrete time domain, without shape differences, can be given respectively by

$$\begin{aligned} x_1(n) &= s(n) + w_1(n) \\ x_2(n) &= s(n - \theta(n)) + w_2(n) \end{aligned} \tag{1}$$

where $\theta(n)$ is the propagation delay between the two signals, $w_1(n)$ and $w_2(n)$ are assumed to be independent, white, zero mean, additive Gaussian noises, of equal variance σ^2.

Once θ(n) is estimated, the MFCV can be simply deduced by MFCV(n) = Δe/θ(n), where Δe stands for the inter-electrode distance, which is taken as 10 mm in the following. The digitization step is processed at the sampling frequency F_s = 1024 Hz. MFCV can be calculated from $\theta(n)$ through

$$MFCV(n) = \frac{F_s.\Delta e}{\theta(n)} \tag{2}$$

where Fs is the sampling frequency and e is the inter-electrode distance.

Next, we describe in detail the way for generating synthetic sEMG signals with predefined TVD functions.

2.2 Delayed Signal Generation

The signals are synthetic ones and are generated according to the following analytic Power Spectral Density (PSD) shape proposed by Shwedyk *et al.* in [18] and written in the following equation as

$$PSD(f) = \frac{k f_h^4 f^2}{\left(f^2 + f_l^2\right).\left(f^2 + f_l^2\right)^2} \tag{3}$$

An example of sEMG PSD shape is given in [5], where the low and high frequency parameters are fixed as f_l = 60 Hz and f_h = 120 Hz, respectively. The parameter k is a normalization factor. The first channel is generated by linear filtering of white Gaussian noise with the impulse response corresponding to this PSD (*i.e.* the inverse Fourier transform of the square root of the previous PSD shape. Once the first channel is generated, its delayed version is created, thanks to the sinc-interpolator [3]:

$$s(n - \theta(n)) = \sum_{i=-p}^{p} \mathrm{sinc}(i - \theta(n)) s(n - i) \tag{4}$$

The parameter p is the filter length and is fixed by p = 40. Finally, both channels are distorted by adding White Gaussian noise at a given signal-to-noise ratio (SNR) level.

3 Proposed Methods

3.1 Maximum Likelihood Estimation

This method was derived in [12]. The estimated TVD can be defined by Eq. 5. Maximize the log-likelihood function is equivalent to minimizing the following expression:

$$\hat{\theta} = \arg\min_{\theta} e_t^2(\theta) \tag{5}$$

where

$$e_t^2(\theta) = \sum_{n=1}^{N} \left(x_2\left(n - \theta(n)\right) - x_1(n)\right)^2 \tag{6}$$

3.2 Polynomial Model

The problem of estimating (n) is the same as estimating the N-dimensional vector $\theta = [\theta(1)\theta(2)\ldots.\theta(N)]$. In the case of TVD polynomial models, this problem, as expressed in Eq. 7, reduces to the estimation of a p + 1-dimensional vector $\Theta = [\theta_0\theta_1\ldots.\theta_p]$.

Thank to the Weierstrass theorem, the TVD may be decomposed up to order p on the canonical polynomial basis as:

$$\theta(n) = \mathrm{F_s} \sum_{k=0}^{p} \theta_k.n^k \tag{7}$$

where F_s is the sampling frequency.

The TVD is thus defined by a p + 1 dimensional vector with parameters $\Theta = [\theta_0\theta_1\ldots.\theta_p]$. In this work, the stochastic optimization technique, called simulated annealing was used to solve the optimization. We detail below this optimization technique.

3.3 Stochastic Optimization

The technique known as simulated annealing is motivated by an analogy to annealing in solids. The idea comes from a paper published by Metropolis *et al.* 1953 [15]. The algorithm in this paper simulates the cooling of the material in a heat bath. This is a process known as annealing. If a solid is heated to melting point and then cooling it, the structural properties obtained for the solid will depend on the cooling rate. If the liquid is cooled slowly enough, large crystals will form. However, if the liquid is rapidly cooled, the crystals contain imperfections. The cooling rate is a critical parameter in the process of crystallization. Metropolis algorithm proposes to simulate the material as a particle system and simulates the cooling process by progressively lowering the temperature of the system until it converges to a stable state frozen. The cooling rate is a critical parameter in the process of crystallization. In 1983, Kirkpatrick *et al.* [8] took up the idea of the Metropolis algorithm and applied to optimization problems. The idea is to use simulated annealing to search for feasible solutions and converge to an optimal solution. A Markov process is used to sample the "objective" function $l\left(\Theta^{(k)}\right)$, seeking a new solution generated in a neighborhood of the current solution, with the objective of minimizing this function. The exploration of the solution space is controlled by a Boltzmann distribution parameter T [4] which describes the behavior of a system "thermodynamic equilibrium" at a certain temperature T. The simulated annealing method, iterative, based on the rule of acceptance Metropolis-Hastings of accepting or refusing a vector solution especially in a function of temperature T. A significant temperature allows to temporarily accept the solutions that move away from the minimum. This allows us to explore more broadly the solution space and thus out of a local minimum. The equilibrium is then achieved with slowly decrease in temperature. For a temperature T and iteration, the algorithm is as follows:

1. Generate vector $\Delta l = l(\Theta^{(k)}) - l(\Theta^{(k-1)})$
2. Apply the Metropolis acceptance rule that involves:
   - If $\Delta l \leq 0$: accept $\Theta^{(k)}$, increment k then iterating step 1
   - If $\Delta l > 0$: accept $\Theta^{(k)}$ with probability $P = e^{\left(-\frac{\Delta l}{T}\right)}$:
     Randomize a random number R between 0 and 1 according to a uniform law.
     if $R \leq P$: accept $\Theta^{(k)}$; increment k and go to step 1.
     If $R > P$: refuse $\Theta^{(k)}$ and go to step 1.

Simulated annealing parameters. The implementation of the simulated annealing procedure requires the setting of several parameters, which play a decisive role in its efficiency.

1. Research neighborhood
   The search for a new solution $\Theta^{(k)}$ is done in the neighborhood of the current solution $\Theta^{(k-1)}$. We have used for the generation of $\Theta^{(k)}$ a normal distribution centered on $\Theta^{(k-1)}$.
   $$\Theta^{(k)} = \Theta^{(k-1)} + \delta \tag{8}$$
   where δ Is an agitation vector generated by a normal distribution $\mathcal{N}(0, \sigma^2)$. In order to unify the standard deviation σ for all the parameters of the vector Θ, we propose to normalize the orthogonal basis of Legendre polynomial. It makes it possible to produce variations of the parameters θ_i of the same order. For a large exploitation of the search space, we take an initial σ of the order of 1/4 of the range of variation. σ decreases with decreasing temperature to obtain a better accuracy of the results.
2. Initial temperature
   It must be high enough so that most degradation are authorized at the beginning of the procedure to allow the location of the region of the global minimum.
   An study [2,16] has shown that an initial value of the temperature of the order of that of the initial "objective" function leads to good results. Thus, the proposed initialization is defined by:
   $$T_0 = \frac{l\left(\Theta^{(0)}\right)}{A} \tag{9}$$
   where $l\left(\Theta^0\right)$ Represents the value of the "objective" function for the initial solution Θ^0 and A is a parameter to be fixed.
3. Diagram of temperature decrease
   It represents the number of solutions tested before applying the diagram of temperature decrease. It is assumed to be constant for all temperature levels. If this length is too small, the exploration of the search space may be too partial, whereas a too large value may have the effect of slowing down or even blocking the search.
   $$T_k = T_{k-1}.C \tag{10}$$
   with $0 < C < 1 (C = 0.95)$.

4. Length of temperature bearing
   The temperature is lowered slowly by marking bearings. The temperature change of the bearing T_k to $T_{(k-1)}$ is carried out according to a given decay pattern. The most commonly used schemes are the arithmetic, geometric, logarithmic or exponential laws.
5. Criteria for stopping the program
   To stop the program, several criteria can be used, separately or often together:
   The temperature becomes lower than a given value.
   The function "objective" ceases to evolve during the decrease of the temperature.
   The non-evolution of the current solution on D consecutive steps.

Setting the parameters of simulated annealing. The setting of the simulated annealing algorithm is done empirically. Several tests are made to arrive at the right parameters which give the best results. These parameters (described in Sect. 3.3) are:

1. The initial search point, chosen equal to $\Theta^{(0)} = [1, 1, \ldots, 1]$ because the "objective" function has a high value for this point. The stirring vector δ of law $\mathcal{N}(0, \sigma^2)$ is initialized with $\sigma = 1$ (depending on the problem data, F_s and distance IE). The standard deviation decreases with the temperature according to: $\sigma_k = 0.98$ (k is the index of the temperature bearing).
2. The temperature parameters: the initial temperature is determined by Eq. 9 with the fixed parameter $A = 0.75$. The diagram of temperature decrease used is a geometric law described in Eq. 10, with C is a fixed parameter $C = 0.95$, because it allows to have a rapid decrease at the beginning of the optimization and slow close to the convergence.
3. The length of the bearing temperature, set at 100 iterations.
4. A counter to stop the program, set to zero at the beginning. The search stops when the counter reaches a certain threshold ($D = 10$). At the end of a stage, the counter is incremented if the current solution does not evolve and it is reset if the quality of the best solution has evolved during the bearing.

The simulated annealing method has the advantage of being flexible with respect to evolution of the problem and easy to implement. It has produced excellent results for a large number of problems, most often large. On the other hand, this algorithm has the disadvantage of having a high number of parameters (initial temperature, decrease in temperature, duration of temperature steps, etc.) whose settings often remain fairly empirical.

4 Results and Discussions

In this section, we detailed statistical study of the performances of the proposed methods. First, the statistical tool are detailed. Then, the simulation strategy is described. The results of the proposed methods compared with the CRLB are also detailed.

4.1 Statistical Tool

To evaluate the performance of the estimators, the useful tool are the normalized bias and the root mean square error (RMSE). The variance of these estimators are also useful to compare with the CRLB.

The normalized bias is expressed by:

$$Bias(\widehat{\theta}(n)) = \frac{\left|E\left[\widehat{\theta}(n)\right] - \theta(n)\right|}{\theta(n)} \tag{11}$$

And the instantaneous RMSE is defined by:

$$RMSE(\widehat{\theta}(n)) = \sqrt{E(\left(\widehat{\theta}(n) - \theta(n)\right)^2)} \tag{12}$$

where $\widehat{\theta}(n)$ is the estimator of $\theta(n)$. The symbol $E[.]$ denote the expectation operator.

4.2 Monte-Carlo Simulation

A Monte-Carlo simulation with 150 independent runs was performed for each signal to noise ratio (SNR) value in order to study the noise impact of these estimators. In this work, two synthetic sEMG signals have the same value of SNR = 10, 20 dB respectively. Duration of the signals is 1 s, the sampling frequency was set as $F_s = 1024$ Hz and the inter-electrode distance is $\Delta e = 10$ mm.

4.3 Simulation Results

Inverse sinusoidal model. This model has been previously proposed in [9]. It takes into account reasonable physiological variations of MFCV that may be encountered during dynamical exercise situations. In particular, the minimum and maximum MFCV values are $2\,\mathrm{m.s^{-1}}$ and $8\,\mathrm{m.s^{-1}}$ respectively. The maximum acceleration value is $2.5\,\mathrm{m.s^{-2}}$. One period of the sine wave is considered corresponding to 1 s observation duration or to equivalently 1024 data samples.

$$\theta(\mathrm{n}) = \mathrm{F_s}\frac{10.10^{-3}}{5 + 3\sin\left(0.2\mathrm{n}2\pi/\mathrm{F_s}\right)}. \tag{13}$$

Applying the model 13 on the delay $\theta(n)$. The approximations $\theta_a(n)$ of $\theta(n)$ for different orders are shown in Fig. 1. The resulting parameters up to order 9 are: $\Theta = [4.18;\ 1.21;\ -0.09;\ -1.01;\ 0.33;\ 0.15;\ 0.24;\ 0.07;\ -0.05;\ -0.06]$.

We propose to estimate the delay with an order $P = 7$. This choice is justified by a compromise between an acceptable approximation error and a lowest possible order. An mean square error (MSE), between the theoretical delay $\theta(n)$ and $\theta_a(n)$ was set at 5.10^{-2}. The estimation results are shown in Fig. 2 (150 simulations of Monte Carlo).

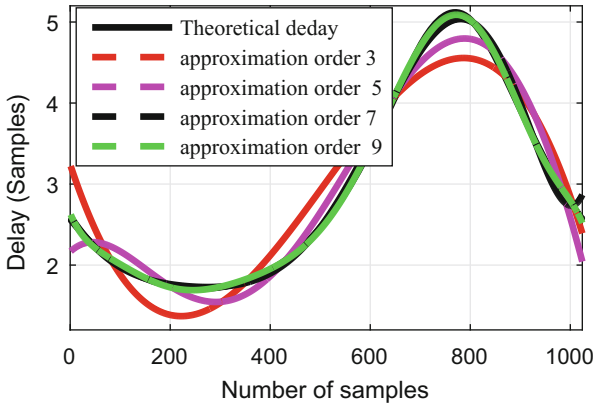

Fig. 1. $\theta(n)$, and and its approximations $\theta_a(n)$ by the model 7 for P = 3, 5, 7 and 9.

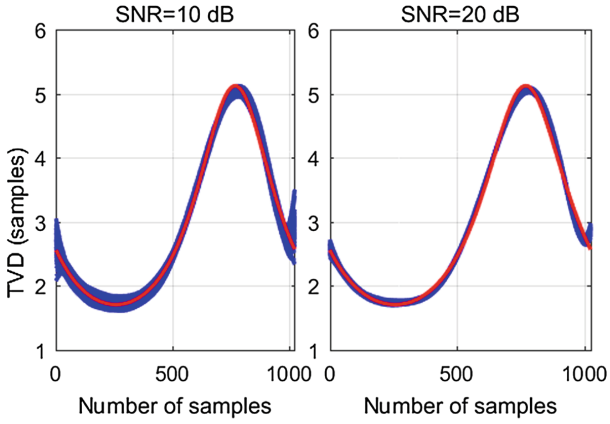

Fig. 2. Delay theoretical (red) $\theta(n)$ and its estimate (blue) with P = 7, (a) SNR = 10 dB, (b) $SNR = 20$ dB. (Results of 150 Monte Carlo simulation, N = 1024 samples, $F_s = 1024$ Hz, $\Delta e = 10$ mm) (Color figure online)

Indeed, the simulated annealing algorithm estimates the approximation of the delay $\theta_a(n)$ of $\theta(n)$. There are two types of errors: estimation errors (Fig. 3) and errors due to the applied model (Fig. 4).

The bias shown in Fig. 5 represents the total error committed (including the modeling error). This bias is low (<5%). For $SNR = 20$ dB, this bias is independent of the SNR because the error due to the estimate is negligible compared to the error due to the model. Increasing the P order reduces modeling errors, but the difficulty of the estimation problem increases.

The MLE method using the model (7) is compared with a method that exploits the information of the phase of the time-frequency plane (phase coherency).

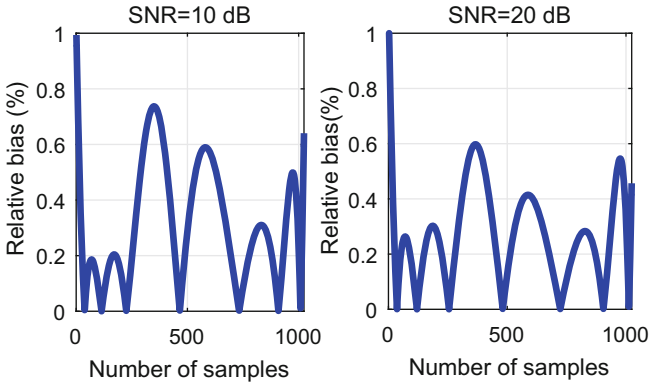

Fig. 3. Relative bias (relative to $\theta_a(n)$): $SNR = 10\,\text{dB}$, (b) $SNR = 20\,\text{dB}$

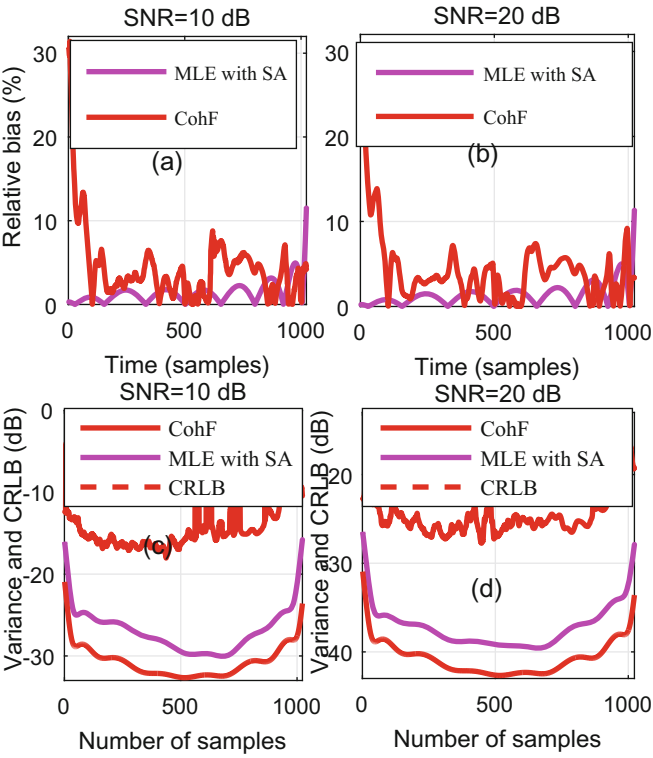

Fig. 4. Statistical results for two estimation methods: MLE (with simulated annealing and an order 7) and phase coherency (CohF) [17] (time-frequency plane calculated on windows of 256 samples (0.25 s), number of fft = 1024. (a), (b) Relative bias (relative to the theoretical delay ($\theta(n)$); (c), (d) variance and CRLB, $F_s = 1024\,\text{Hz}$, $\Delta e = 10\,\text{mm}$.

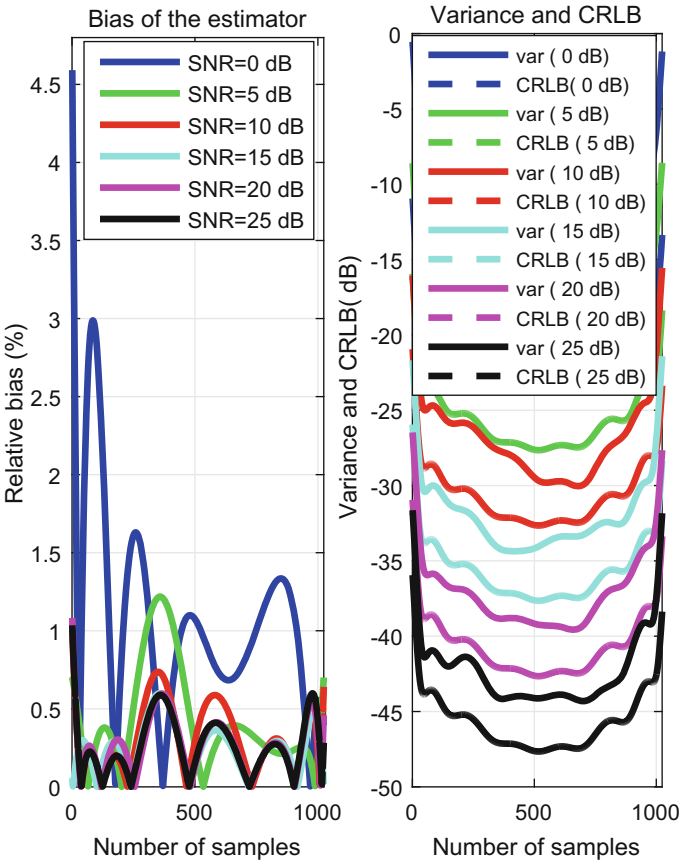

Fig. 5. Statistical results of the $\widehat{\theta}(n)$: (a) relative bias (relative to $\theta_a(n)$ approximation of order 7 of $\theta(n)$, (b) variance (continuous curve) compared with CRLB (discontinuous curve) and each color corresponds to an SNR, 150 runs of Monte-Carlo simulation, N = 1024 samples, $F_s = 1024\,\text{Hz}$, $\Delta e = 10\,\text{mm}$. (Color figure online)

For the method MLE optimized by simulated annealing, the estimator is weakly biased (a very low relative bias <1%). Moreover, the variance of the estimator is very close to the CRLB (a difference of 3 dB). In general, the estimator can be said to be effective.

The MLE method yielded good results with respect to the Fourier Coherency (CohF) method. For CohF method, the estimator is biased. Therefore, the variance of the estimator is very far from the CRLB (a difference of 20 dB). This method is very sensitive to noise (limited at $SNR = 10\,\text{dB}$).

5 Conclusions

In this paper, we have investigate the TVD estimator using the parametric approach. First, the polynomial model for TVD have been proposed. Second, MLE

estimation of the parameter model have been performed using the optimization technique called simulated annealing. The simulation results shown that the MLE method combined with simulated annealing technique is an unbiased estimator. It has a variance 3 dB higher than the CRLB. SA technique also outperformed compared with the CohF method [17]. To increase the performance of estimation, we have to increase the polynomial order of TVD model, but the execution time of also increase. In the future, we will compromise between the execution time and the order of the polynomial model. We will also investigated an other optimization technique in order to improve the performance of the estimator. The PSD shapes of sEMG signals will be also considered in order to take into account the fatigue effect.

Acknowledgment. The authors would like to thank the Posts and Telecommunications Institute of Technology, Ho Chi Minh City Branch for funding this research in project 03-*HV*-2017-*RD*-*CB*2.

References

1. Allen, D.C., Arunachalam, R., Mills, K.R.: Critical illness myopathy: further evidence from muscle-fiber excitability studies of an acquired channelopathy. Muscle Nerve **37**(1), 14–22 (2008)
2. Athier, G., Floquet, P., Pibouleau, L., Domenech, S.: Synthesis of heat-exchanger network by simulated annealing and NLP procedures. AIChE J. **43**(11), 3007–3020 (1997)
3. Chan, Y., Riley, J., Plant, J.: Modeling of time delay and its application to estimation of nonstationary delays. IEEE Trans. Acoust. Speech Signal Process. **29**(3), 577–581 (1981)
4. Dréo, J., Siarry, P.: Métaheuristiques d'optimisation vues sous l'angle de l'échantillonnage de distribution. J. Européen des Systèmes Automatisés **42**(1), 9 (2008)
5. Farina, D., Merletti, R.: Comparison of algorithms for estimation of EMG variables during voluntary isometric contractions. J. Electromyogr. Kinesiol. **10**(5), 337–349 (2000)
6. Farina, D., Pozzo, M., Merlo, E., Bottin, A., Merletti, R.: Assessment of average muscle fiber conduction velocity from surface EMG signals during fatiguing dynamic contractions. IEEE Trans. Biomed. Eng. **51**(8), 1383–1393 (2004)
7. Gerdle, B., Ostlund, N., Grnlund, C., Roeleveld, K., Karlsson, J.S.: Firing rate and conduction velocity of single motor units in the trapezius muscle in fibromyalgia patients and healthy controls. J. Electromyogr. Kinesiol. **18**(5), 707–716 (2008)
8. Kirkpatrick, S., Gelatt, C.D., Vecchi, M.P.: Optimization by simulated annealing. Science **220**(4598), 671–680 (1983)
9. Leclerc, F., Ravier, P., Buttelli, O., Jouanin, J.C.: Comparison of three time-varying delay estimators with application to electromyography. In: 2007 15th European Signal Processing Conference, pp. 2499–2503, September 2007
10. Leclerc, F., Ravier, P., Farina, D., Jouanin, J.C., Buttelli, O.: Time-varying delay estimation with application to electromyography. In: 2008 16th European Signal Processing Conference, pp. 1–5, August 2008

11. Luu, G.T.: Contributions à lestimation de la vitesse de conduction des signaux électromyographiques. Ph.D. dissertation, Orleans University (2013)
12. Luu, G.-T., Ravier, P., Buttelli, O.: Comparison of maximum likelihood and time frequency approaches for time varying delay estimation in the case of electromyography signals. In: Biomedical Engineering International Conference (BMEiCON), pp. 1–5 (2012)
13. Merletti, R., Knaflitz, M., De Luca, C.J.: Myoelectric manifestations of fatigue in voluntary and electrically elicited contractions. J. Appl. Physiol. **69**(5), 1810–1820 (1990). http://jap.physiology.org/content/69/5/1810
14. Merletti, R., Conte, L.R.L.: Surface EMG signal processing during isometric contractions. J. Electromyogr. Kinesiol. **7**(4), 241–250 (1997)
15. Metropolis, N., Rosenbluth, A.W., Rosenbluth, M.N., Teller, A.H., Teller, E.: Equation of state calculations by fast computing machines. J. Chem. Phys. **21**(6), 1087–1092 (1953)
16. Pibouleau, L., Domenech, S., Davin, A., Azzaro-Pantel, C.: Expérimentations numériques sur les variantes et paramètres de la méthode du recuit simulé. Chem. Eng. J. **105**(3), 117–130 (2005)
17. Ravier, P., Farina, D., Buttelli, O.: Time-varying delay estimators for measuring muscle fiber conduction velocity from the surface electromyogram. Biomed. Signal Process. Control **22**, 126–134 (2015)
18. Shwedyk, E., Balasubramanian, R., Scott, R.N.: A nonstationary model for the electromyogram. IEEE Trans. Biomed. Eng. **BME–24**(5), 417–424 (1977)
19. Yaar, I., Niles, L.: Muscle fiber conduction velocity and mean power spectrum frequency in neuromuscular disorders and in fatigue. Muscle Nerve **15**(7), 780–787 (1992). https://doi.org/10.1002/mus.880150706